Comments on the alpha -peak shapes for relaxation in supercooled liquids

1991 J. Phys.: Condens. Matter 3 5047

(http://iopscience.iop.org/0953-8984/3/26/022)

J. Phys.: Condens. Matter 3 (1991) 5047–5071. Printed in the UK

Comments on the α-peak shapes for relaxation in supercooled liquids

M Fuchs, W Götze†, I Hofacker and A Latz

Physik-Department, Technische Universität München, D-8046 Garching, Federal Republic of Germany

Received 31 January 1991, in final form 21 April 1991

Abstract. The α-peak master functions as obtained within the mode coupling theory for the supercooled liquid dynamics near the glass transition singularity are discussed. Double peak phenomena are found as a generic feature of the theory related to the self crossing of the transition hypersurface. They lead to two scenarios for liquid to glass transitions characterized by α'–α-peak pairs and by α-resonances accompanied by γ-peaks. An efficient numerical procedure is developed for the solution of the non-linear scaling equations for the master functions. A schematic three component model is used to fit quantitatively the dielectric loss spectra of polyvinylacetate, ortho-terphenyl, $CaKNO_3$ and poly propylene glycol, which all deviate strongly from the Kohlrausch decay pattern. The model yields also triple resonances of α–γ–δ-peaks.

1. Introduction

The α-relaxation process is a characteristic feature of the dynamics of those supercooled liquids which exhibit a glass transition. It describes the slowest part of the autocorrelation functions $\Phi(t)$ of variables like mechanical stress, dielectric polarization or density fluctuations. It shows up as a low frequency spectrum $\chi''(\omega)$ in various susceptibilities as measured e.g. by dielectric loss spectroscopy and Brillouin or neutron scattering experiments. For a review the reader can consult the books by McCrum *et al* (1967), Wong and Angell (1976) or Brawer (1985). In this article some details of the variation of Φ with time t or of $\chi''(\omega)$ with frequency ω will be considered. Some examples for the α-relaxation stretching phenomena will be quoted and it will be demonstrated that a simple version of the mode coupling theory, to be abbreviated as MCT, can account for the data. For a summary of the MCT the reader is referred to a recent review (Sjögren and Götze 1989).

Stochastic relaxation, as described by the Debye law $\Phi_D(t) = f \exp -(t/\tau)$, implies a decay from 90 to 10% within a time interval of 1.34 decades. Such a relaxation is never observed in glassy materials. Rather the time interval for the specified 80% decay is stretched to much longer values. The stretched exponential function

$$\Phi_K(t) = f \exp -(t/\tau)^\beta \qquad \beta < 1 \tag{1}$$

† Also at: Max-Planck-Institut für Physik und Astrophysik, D-8000 München, Federal Republic of Germany.

0953-8984/91/265047+25$03.50

(Kohlrausch 1854, Williams and Watts 1970, Ngai 1979), is the best of all simple fit formulae for the α-process. The short time part of (1) is a power law decay

$$\Phi(t) = f - (t/\tau)^b + O((t/\tau)^{2b}). \tag{2}$$

This fractal time variation is often observed for dynamical ranges of 2 to 3 decades (von Schweidler 1907, Jonscher 1977). It implies a similar power law decay for the large frequency part of the α-spectrum, $\omega\tau \gg 1$:

$$\chi''(\omega) = f\sin((\pi/2)b)\Gamma(1+b)/(\omega\tau)^b \qquad \chi'(\omega) - \chi_0 = f\cos((\pi/2)b)\Gamma(1+b)/(\omega\tau)^b. \tag{3}$$

The known connections of χ'', χ' and Φ via Fourier transforms have been used. The Debye relaxation resonance $\chi''_D(\omega) = f(\omega\tau)/(1+(\omega\tau)^2)$ has a half width of 1.14 decades. The stretching implies peaks which are much broader. The Kohlrausch law (1) essentially models the stretching via the slowly decaying von Schweidler asymptotic tail (2). If the von Schweidler law and the Kohlrausch law both were valid, one would get $\beta = b$.

Since correlation functions behave regularly for small times, there must be a small time cut-off and a corresponding large frequency limit for the α-process:

$$t_c \ll t \qquad \omega \ll \omega_c = 1/t_c. \tag{4}$$

Often one writes the correlation function as Laplace transform

$$\Phi(t) = f\int_0^\infty d\gamma\rho(\gamma)\exp(-\gamma t). \tag{5}$$

The correlator Φ is represented as a superposition of Debye laws, where $\rho(\gamma)$ is the weight for the relaxation process with decay constant γ. Experiments suggest that $\Phi(t)$ is completely monotonic and therefore $\rho(\gamma) \geqslant 0$. Stretching is equivalent to a broad distribution of rates γ.

The α-relaxation functions depend strongly on control parameters like the temperature T. Often one finds the time temperature superposition principle to be valid:

$$\Phi(t)/f = F(t/\tau). \tag{6}$$

Here F is a master function which shows no, or only weak, T-dependence. The drastic T-dependence enters via the scale τ of the α process. The scaling law (6) is equivalent to similar ones for the susceptibility spectrum

$$\chi''(\omega)/\chi_{\max} = \tilde{\chi}''(\omega\tau) \tag{7}$$

or for the rate distribution

$$\rho(\gamma) = \tilde{\rho}(\gamma\tau). \tag{8}$$

Here again the master functions $\tilde{\chi}''$ and $\tilde{\rho}$ depend on T only smoothly if at all. For the simple fit formulae (1) or (2) the scaling law is equivalent to the temperature independence of the exponents β or b respectively.

Equation (5) suggests the explanation of stretching in disordered materials as parallel relaxation process: with probability $\rho(\gamma)$ there is some complex which relaxes with rate γ (von Schweidler 1907). This picture is quite appropriate for a variety of situations. Exciton line shifts are caused by van der Waals interactions and the distribution of pair distances leads to the distribution of rates γ. One finds (1) with exponent $\beta = 1/2$ (Förster 1949). Assuming different interactions one gets different β (Blumen 1981). Near second order phase transition points a system can be described in a droplet picture. The distribution of droplet sizes yields non-trivial $\rho(\gamma)$ and the critical fractals lead to the Kohlrausch law (1) (Piazza *et al* 1988). There is no obvious reason why the quoted physical mechanisms should be relevant in general to explain the α-process in supercooled liquids. The validity of the scaling law (5) is also an argument against the picture of independently relaxing complexes (Williams and Hains 1972).

The free volume theory (Cohen and Grest 1979) associates the glass transition with a percolation threshold, which is reached upon lowering the temperature to some T_0. T_0 is located near and below the transformation temperature T_g. The critical percolation cluster introduces fractal structures in space and this leads to the Kohlrausch law. Two predictions are made (Cohen and Grest 1981): $\beta \geqslant 1/2$ and for $T \to T_0$ the α-relaxation time τ_α for some relaxation process should be proportional to the relaxation time τ_s for shear motion. There are experiments with β smaller than 0.5 (Williams and Watts 1970, Frick *et al* 1990) and even some with β smaller than $\frac{1}{3}$ (Ngai 1979). Others show a decoupling of relaxation processes in the sense, that τ_α/τ_s increases as fast as τ_s itself for $T \to T_0$ (Ehlich and Silescu 1990, Rössler 1990). There is no experimental evidence for fractal structure in space for $T \approx T_g$.

The Kohlrausch law was derived also for the dynamics of certain spin glass models. A random walk theory produced (1) with the prediction that β should decrease towards 1/3 if the temperature decreases towards some $T_0 < T_g$. The scaling law (6) is predicted to hold if and only if for high temperatures $\beta = 1$ (Campbell *et al* 1988, Flesselles and Botet 1988). Also a master equation approach for the dynamics of the Sherrington–Kirkpatrick spin glass model predicted (1) with a temperature dependent β. In addition an Arrhenius law for τ was obtained (De Dominicis *et al* 1985). Arrhenius laws are invalid for many structural glass formers. On the basis of dynamical light scattering data for $CaKNO_3$ (Pavlatou *et al* 1990) and extensive Brillouin scattering results for propylene carbonate (Börjesson *et al* 1990) was argued against the applicability of theories with T-dependent β for structural glass formers.

Palmer *et al* (1984) pointed out that a broad distribution of rates $\rho(\gamma)$ is expected for hierarchically constrained relaxation processes. One complex transfers the perturbation to the next only after the earlier complex has already relaxed. Unfortunately, so far it has not been possible to substantiate that picture. It is unclear e.g. whether (5) is valid. In any case it is not known whether different processes are ruled by a similar τ or not. No specific form for the function $\Phi(t)$ could be derived; the Kohlrausch law (1) was obtained only from an unmotivated assumption on a fractal distribution for the transfer rates.

2. Examples for α-relaxation susceptibilities

Many experimental data, reviewed by Ngai (1979), show that (1) is a reasonably satisfactory representation of a major part of the α process of a variety of glass formers. This holds also for the relaxation of density fluctuations as detected recently

in the GHz band by neutron spin echo spectroscopy for $CaKNO_3$ (CKN) by Mezei *et al* (1987), for polybutadien (PB) by Richter *et al* (1988) and Frick *et al* (1990), and for ortho-terphenyl (OT) by Petry *et al* (1991). The α-relaxation process, as identified by molecular dynamics for simple model systems has also been fitted well by the Kohlrausch law (Roux *et al* 1989, Signorini *et al* 1990, Barrat *et al* 1990). Let us mention as a particularly convincing confirmation of (1) with $\beta = 0.74$ the measurements of Howell *et al* (1974) for CKN in the temperature interval between 25°C and 54°C ($T_g = 60$°C). The dielectric modulus was tested on a frequency region extending over 4.5 decades. In this manner 95% of the α peak was mapped out.

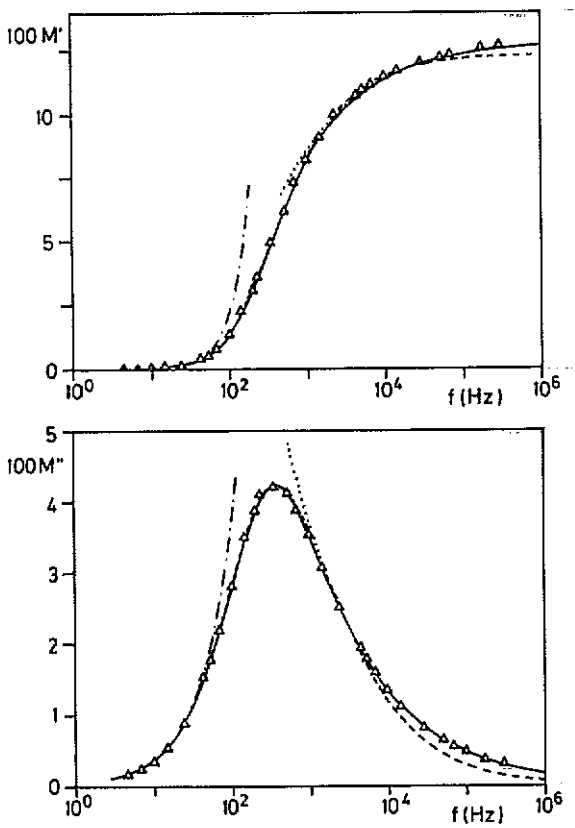

Figure 1. Reactive part M' and absorptive part M'' of the CKN dielectric modulus at 71.4°C (triangles) together with a Kohlrausch fit with exponent $\beta = 0.64$ (broken curves) from Howell *et al* (1974). The dotted curves are von Schweidler asymptotes (2) for exponent $b = 0.44$. The chain curves are fits to the stochastic behaviour $M' \propto \omega^2$, $M'' \propto \omega$. The full curves are MCT results for the model (40) and (41), specified in the text.

In order to judge the relevance of a test of (1) it is important to consider the dynamical window and the part of the process which has been analyzed. Three examples shall be considered in detail to reiterate this statement. Figure 1 reproduces a dielectric modulus of CKN together with a best fit to the Kohlrausch function (Howell *et al* 1974). Formula (1) describes well the upper half and the complete low frequency wing of the α-peak. But it fails to describe the large frequency modulus for $\omega/\omega_{max} > 15$, where $M''/M_{max} < 0.4$. The measured spectrum M'' differs from the Kohlrausch

spectrum by 100% in the one decade window $f \approx 10^5$ Hz. Extrapolation of $M'(\omega)$ to $M_\infty = M'(\omega \to \infty)$ with (1) systematically underestimates the true value for the high frequency modulus M_∞. However the major part of the high frequency wing where $M''/M_{max} < 0.85$ is described well by the von Schweidler law; it follows the data for the 2.5 decade window where $f > 10^3$ Hz (Fuchs *et al* 1990). For the description of the large frequency wing of the α-resonance, formula (2) is superior to (1). Since $b < \beta$, one cannot treat (2) as special limit of (1). The chain curves in figure 1 represent the low frequency asymptotes $M'' = c_0\omega$ and $M' = c_1\omega^2$. Such regular variation is obtained for $\omega \to 0$ for all correlators which have finite moments $c_n = \int_0^\infty \mathrm{d}t\, t^n\Phi(t)$. These moments exist for the Kohlrausch law as well as for the Debye law. The low frequency wing where $M''/M_{max} < 0.4$ is well described by the regular behaviour. The data do not exhibit any small frequency stretching anomaly. The Kohlrausch law has an essential singularity for large times, which results in an essential singularity for the zero frequency susceptibility. The figure shows that measurements in frequency space are not suited to test this implication of (1).

The observations made above are not restricted to the anorganic glass former CKN. Kohlrausch (1854) has already pointed out that his data set with the largest dynamical window exhibited systematic deviations from his fit formula (1). Also, Williams and Hains (1972) noticed small but systematic discrepancies between fit and data. Figure 2 shows the effect for some of their measurements obtained for the organic glass former OT. Figure 3 shows an α-resonance for polyvenyl acetate (PVA) measured by Ishida *et al* (1962). The organic glass former OT and the polymer PVA also show that the Kohlrausch fit works for the upper part of the resonance. It describes the low frequency wing in the same manner as a non-stretched relaxation function and it fails for the large frequency wing of the peak. In both examples the von Schweidler law is an adequate description of the dynamics for $\omega/\omega_{max} \gg 1$.

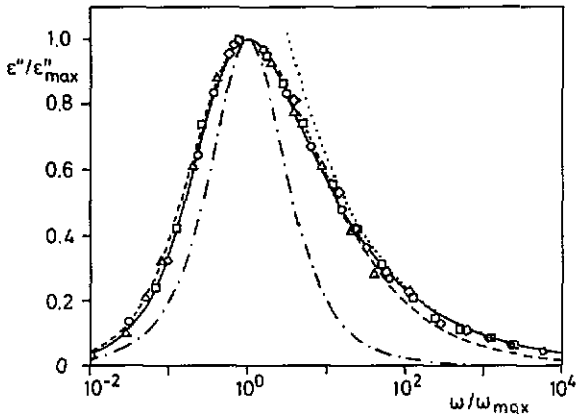

Figure 2. Dielectric loss data measured for OT with 4.2% anthrone by Williams and Hains (1972) replotted as $\epsilon''/\epsilon_{max}$ versus ω/ω_{max} diagram. Symbols, temperatures in K and f_{max} in Hz are the following: ○, 255.5, 9.5; □, 258.6, 40; ◇, 263.0, 320; △, 267.1, 2.4 ×10³. The broken curve is a Kohlrausch spectrum with exponent $\beta = 0.55$ and the dotted one is the von Schweidler asymptote (2) with $b = 0.41$. The chain curve is the Debye resonance. The full curve is a MCT result for model (40) and (41), specified in the text.

There is no consensus in the literature concerning the question of which part

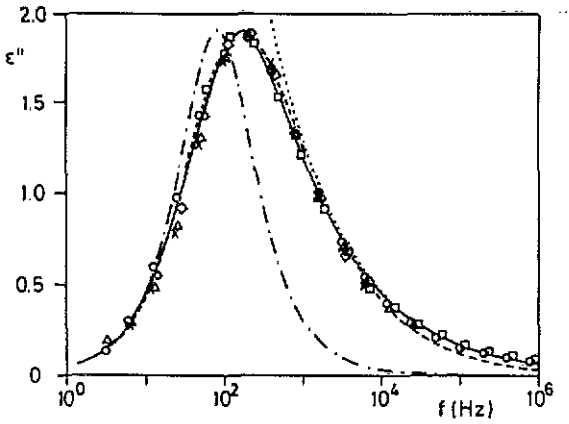

Figure 3. Dielectric loss data measured for PVA by Ishida *et al* (1962), replotted as ϵ''/ϵ_0 versus f/f_0 diagrams. The units ϵ_0, f_0 are maximum value and resonance position for the 62.5°C data, denoted by circles. The squares refer to the data for 53.5° (f_{max} = 8.8Hz), diamonds to 70.0° (f_{max} = 1.2 x 10^3Hz), triangles to 77.0° (f_{max} = 5.5 x 10^3Hz), crosses to 83.5° (f_{max} = 2.6 x 10^4Hz). The broken curve is a Kohlrausch spectrum with β = 0.58 and the dotted one is the von Schweidler asymptote with b = 0.44. The chain curve is a Debye resonance shifted to low frequencies. The full curve is a MCT result for model (40) and (41), specified in the text.

of the high frequency spectrum should be accounted for as an α-process and which should be attributed to some other dynamical feature. There is no precise purely empirical definition of the cut-off frequency ω_c in (4). Therefore one cannot rule out that ω_c is so small that the spectral parts of the high frequency α-peaks in figures 1–3, where (1) is in contradiction to experiment, is excluded from the α-process. In our article this position is not taken for the following reasons. Figures 2 and 3 exemplify the validity of the scaling law (6)–(8). This shows that data for various frequencies and temperatures are tightly connected. It does not seem meaningful to attribute parts of spectra which are so closely connected, as required by the time temperature superposition principle, to different physical processes. Data obeying (6)–(8) presumably refer to one cooperative phenomenon (Williams and Hains 1972). This argument does not apply to the quoted CKN data, since the α-scaling law (7) is not valid in the temperature range discussed in figure 1 (Howell *et al* 1974). The validity of the von Schweidler law (2) over more than two decades frequency interval, shown in figures 1–3, appears also as an argument against dividing the window under consideration into two parts by introducing ω_c. In any case, ω_c would be located at least six decades below the band of phonon excitations or molecular vibrations. Hence ω_c is not connected with short time transient effects. The only physical process proposed so far for non-α-dynamics in the mesoscopic regime under discussion is β-relaxation. One has to remember that β-relaxation scales differently from α-relaxation when changing T. Let ω_α and ω_β denote the respective resonance positions. The ratio $\omega_\alpha/\omega_\beta$ decreases strongly with decreasing T (McCrum *et al* 1967, Wong and Angell 1976, Brawer 1985). Hence, a possible disturbance of α-relaxation by β-relaxation should decrease upon lowering T. The time temperature superposition principle (6)–(8) anticipates that such disturbances have disappeared already. Demonstrating the scaling law (7) in figures 2 and 3 means that no β-process is detectable in those data. Lowering the temperature in CKN to 65.3°C or 60.1°C implies shifts of ω_α by more

than a factor of 10, but there is no indication that the discrepancy between data and a Kohlrausch fit decreases (Howell *et al* 1974), nor does the interval for a successful von Schweidler fit shrink (Fuchs *et al* 1990).

The free volume theory brings out that (1) terminates at small (t/τ) and crosses over to Debye relaxation (Cohen and Grest 1981). Thus the true susceptibility spectrum is predicted to fall below the high frequency tail $\chi'' \propto 1/\omega^{\beta}$ of the Kohlrausch fit if $\omega \gg \omega_{\alpha}$ and this is is just the opposite of what is found in the experiments of figures 1–3.

The low frequency dielectric loss spectrum of polypropylene glycol (PPG) exhibits a double peak. A large peak at some frequency ω_{α} is accompanied by a small one at position $\omega_{\alpha'}$ where the latter frequency is several orders of magnitude smaller than the former (Baur and Stockmayer 1965, Alper *et al* 1976, Johari 1986, Fu *et al* 1991). Also in dynamic Kerr effect measurements (Beevers *et al* 1979) this phenomenon can be seen. Figure 4 reproduces a representative example of the dielectric loss spectra. A double peak pattern was also observed for the shear modulus of PB rubber with a bimodal molecular weight distribution (Sidorovich *et al* 1974) and for Polyisoprene with a narrow molecular weight distribution (Adachi and Kotaka 1984, 1985, Imanishi *et al* 1988). In the latter the intensity of the low frequency peak is higher than that of the high frequency one. Again the time temperature superposition principle is used to argue that both peaks do not represent different phenomena but rather are two facets of the same α-phenomenon. The scaling law (5) implies, for example, that $\omega_{\alpha}/\omega_{\alpha'}$ should be temperature independent even though ω_{α} and $\omega_{\alpha'}$ shift strongly with T. It is difficult to test this law since the spectra extend over such huge dynamical windows as shown in figure 4. Baur and Stockmayer (1965), Sidorovich *et al* (1979), Alper *et al* (1976) and Adachi and Kotaka (1984) confirmed (5). But Beevers *et al* (1979) and Johari (1986) report a temperature dependence of $\omega_{\alpha}/\omega_{\alpha'}$. However, the variation of $\omega_{\alpha}/\omega_{\alpha'}$ in the latter work is much smaller than the variation of ω_{α} and $\omega_{\alpha'}$ themselves. Therefore it seems legitimate to consider the violations of the strict scaling (7) as the expected small temperature variations of the master functions F, $\tilde{\chi}$ or $\tilde{\rho}$. In any case the extensive measurements of Fu *et al* (1991) confirm the scaling law as shown in figure 5. The broken curve in figure 5 is a fit of the double peak by a sum of two Kohlrausch functions. Both peaks exhibit the usual stretching features. The Kohlrausch fit fails for the large frequency data in the same way as discussed above in connection with figures 1–3. The double peak phenomenon is experimental evidence against simple few-parameter fits for the α-relaxation process in glassy materials.

3. Mode coupling theory of the α-process

3.1. Glass transition singularities

For the purposes of this paper it its sufficient to adopt a formal point of view and consider the MCT as a mathematical model for the dynamics of a many particle system. The model is defined by equations of motion for a set of M correlators $\Phi_q(t)$, $q = 1,...,M$, which are normalized by $\Phi_q(t=0) = 1$. The latter describe the dynamics in a statistical manner. The essential piece of the formalism is the mode coupling functional $\mathcal{F}_q$, which is given by M polynomials of the M variables Φ_k. The various coefficients of the polynomials are the coupling constants of the theory. They are combined to a vector V in some N-dimensional control parameter space $\mathcal{K}$. The

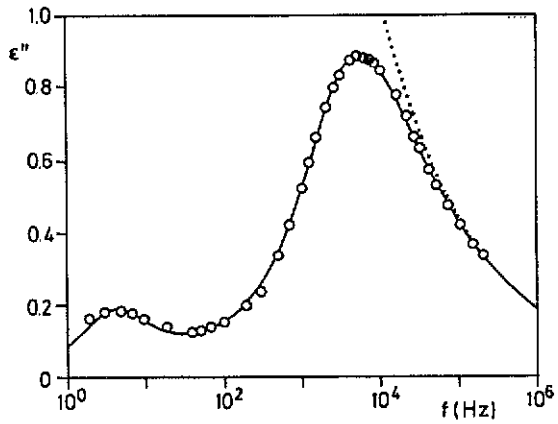

Figure 4. Dielectric loss of PPG at T=223.7 K measured by Johari (1986) (circles). The full curve is a MCT result calculated for the schematic model (40) and (41), specified in the text. The dotted curve is the corresponding von Schweidler asymptote (2) with exponent $b = 0.38$.

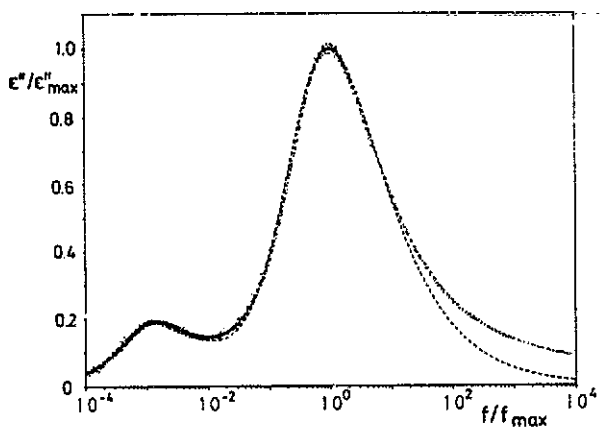

Figure 5. Scaling plot $\epsilon''/\epsilon_{max}$ versus ω/ω_{max} of the measurements of Fu (1990) and Fu *et al* (1991) for PPG. The temperature range extends from 219 K to 358 K and the scaling frequency ω_{max} varies between 0.7 Hz and 2.4×10^6 Hz. The broken curve is the sum of two Kohlrausch functions with exponents $\beta = 0.57$, $\beta' = 0.70$.

components of $\boldsymbol{V}$ are non-negative. The state of the system is specified by $\boldsymbol{V}$. The equations of motion determine the unique solution $\Phi_q(\boldsymbol{V}, t)$ for every $\boldsymbol{V}$.

In applications to simple liquids the index q is a discretized wave vector modulus. The correlators refer to the ones for the density fluctuations ρ_q: $\Phi_q(t) = \langle \rho_q^*(t)\rho_q \rangle / \langle |\rho_q|^2 \rangle$. In this case the polynomials consist of quadratic terms only,

$$\mathcal{F}_q(\boldsymbol{V}, f_k) = \tfrac{1}{2} \sum_{kp} V(q;k,p) f_k f_p, \tag{9}$$

where the vertices $V(q;k,p) \geqslant 0$ are given by the structure factor of the system (Bengtzelius *et al* 1984). In other applications also linear and cubic terms enter the polynomials $\mathcal{F}_q$. The vector $\boldsymbol{V}$ is a smooth function of physical control parameters like the temperature T. So the system is described by a path $T \rightarrow \boldsymbol{V}(T)$. Upon lowering T the path runs from the weak coupling to the strong coupling region.

The space K consists of three sets. There is the open small coupling region of liquid states D_L; for $V \in D_L$ one gets $\Phi_q(t \to \infty) = 0$. There is the open set of ideal glass states D_G. For $V \in D_G$ the glass form factor $f_q(V) = \Phi_q(t \to \infty)$ is a smooth positive function of V and it is smaller than unity. The $(N-1)$-dimensional set D_C of glass transition singularities contains the singular points V_c of $f_q(V)$. The form factor is a solution of the M coupled implicit equations:

$$\frac{f_q}{1-f_q} = \mathcal{F}_q(V, f_k) \qquad 0 \leqslant f_q < 1,\ q = 1, ..., M. \tag{10}$$

If there are several solutions one gets the long time limit $f_q(V)$ from the maximum property: $f_q \leqslant f_q(V)$. The set D_C is formed by bifurcation points of (10). These are located, where the stability matrix $C_{kp} = (\partial \mathcal{F}_k / \partial f_p)(1-f_p)^2$ has an eigenvalue unity. The stability matrix has a non-degenerate maximum eigenvalue $E(V)$, where $E(V) < 1$ for $V \in D_G$. An $(N-1)$-dimensional bifurcation hypersurface $\mathcal{H}$ in K is obtained by

$$E(V_c) = 1. \tag{11}$$

The set D_C is a subset of $\mathcal{H}$, which is constructed with the aid of the mentioned maximum property.

Upon lowering T the path runs from D_L to D_G; it crosses $\mathcal{H}$ at some singularity V_c for $T = T_c$. The temperature T_c is the idealized liquid to glass transition temperature. Generically, $\mathcal{H}$ can be specified near V_c by an implicit equation $\sigma(V) = 0$. Here $\sigma(V)$, the separation parameter, is a smooth function of V so that: $\sigma < 0$ if $V \in D_L$, $\sigma > 0$ if $V \in D_G$. One can expand $\sigma(V(T)) = C_T(T_c - T)/T_c$, where $C_T > 0$ is a constant in leading order for $T \to T_c$. The asymptotic behaviour of the form factor reads

$$f_q = f_q^c + C h_q \sqrt{\sigma} + O(\sigma) \qquad \sigma \to +0. \tag{12}$$

Here $C > 0$. $f_q^c > 0$ is the form factor at the singularity V_c. The critical amplitude $h_q > 0$ is obtained from the stability matrix at V_c.

The dynamics outside the microscopic transient regime is specified by two smooth functions of V. The microscopic time scale $t_0(V)$ connects the mathematical time with the details of the motion for short times. The exponent parameter $\lambda(V)$, obeying $1/2 \leqslant \lambda < 1$, characterizes the position of V_c on $\mathcal{H}$. In leading order calculations for $T \to T_c$ both functions can be treated as constants. Parameter λ determines the two critical exponents $0 < a < 1/2$ and $0 < b \leqslant 1$ of the theory by $\Gamma(1-a)^2/\Gamma(1-2a) = \lambda = \Gamma(1+b)^2/\Gamma(1+2b)$. There appear two critical time scales which quantify the slowing down of the dynamics for $T \to T_c$:

$$t_\sigma = t_0/|\sigma|^{1/2a} \qquad t'_\sigma = t_0/|\sigma|^\gamma \qquad \gamma = (a^{-1} + b^{-1})/2. \tag{13}$$

These two time scales govern the sensitive dependence of the low frequency spectra on T for small $T - T_c$. The subtle low frequency singularities of the spectra for $\sigma \to 0$ are proposed to describe the experimental findings of the dynamics of supercooled liquids. The dynamics on scale t'_σ is called α-process and the one on scale t_σ is referred to as β-process. Both processes are intimately connected and they overlap on the time interval $t_\sigma \ll t \ll t'_\sigma$. In this paper only those formulae and concepts are mentioned which are necessary to formulate the following new results. A more detailed summary of the MCT with a reference list to the original papers can be found elsewhere (Götze 1991).

3.2. General results for the α-process

The equations of motion of the MCT (Bengtzelius *et al* 1984) imply (Götze 1987):

$$\lim_{\sigma \to -0} \Phi_q(\tilde{t} t'_\sigma) = F_q(\tilde{t}). \tag{14}$$

This is equivalent to

$$\Phi_q(t) = \tilde{F}_q(t/\tau) \qquad t_\sigma \ll t \qquad \tau = t'_\sigma \tag{15}$$

where $\tilde{F}$ is a smooth function of V, which approaches F for $V \to V_c$. In leading order $\tilde{F} = F$, for $T \approx T_c$. Function F_q obeys (Götze 1984, 1987)

$$F_q(\tilde{t}) = f_q^c - B h_q \tilde{t}^b + O(\tilde{t}^{2b}). \tag{16}$$

Here f_q^c, h_q have the same meaning as in (12); b is determined by λ as mentioned above, and $B > 0$ is also given by λ. The full function F_q is a solution of a non-linear equation solely fixed by the mode coupling functional for $V = V_c$ (Götze 1987). The latter shall be rewritten in the form of an integro differential equation:

$$F_q(t) = m_q(t) - \frac{\mathrm{d}}{\mathrm{d}t} \int_0^t dt' m_q(t - t') F_q(t') \tag{17}$$

$$m_q(t) = \mathcal{F}_q(V_c, F_k(t)). \tag{18}$$

In applications of the MCT, autocorrelation functions Φ_x formed with variables X of even time inversion symmetry are reduced to polynomials of the correlators $\Phi_q(t)$:

$$\Phi_x(t) = \mathcal{F}_x(V, \Phi_k(t)). \tag{19}$$

In the α-regime one can write $V = V_c$. Obviously one gets from (19)

$$\Phi_x(t) = F_x(t/\tau), \tag{20}$$

where F_x is independent of T in the limit $T \to T_c^+$. One gets also formulae like (12) and (16), where merely the quantities f_q, h_q have to be replaced by other numbers f_x, h_x, reflecting the properties of variable X. These results apply e.g. to the dielectric function or modulus, where X is the dipole moment or the fluctuating force on the currents respectively. For qualitative discussions of the dielectric loss spectra or of the dielectric modulus one can directly use the properties of the $\Phi_q(t)$.

An efficient way to partly solve (17) is the extension of (16) to an asymptotic series in powers of t^b. Numerical work indicates that this series has a finite non-zero radius of convergence. The solution of (17) is uniquely determined for all t by the solution within any small initial time interval $0 < t < \epsilon$ (Hofacker 1990). One can show $F > 0$ and $\dot{F} < 0$ (Götze and Sjögren 1987a). Generically the Kohlrausch law is not a solution of (17).

Equations (15) and (20) are the time temperature superposition principle (5), which is obtained within the MCT as asymptotic law for temperatures decreasing towards T_c. The time t'_σ is the scale for the α-processes. As cut-off time t_c in (4)

the scale t_σ is found. It is not the microscopic scale t_0; rather it is a critical quantity which characterizes the center of the β-process. The von Schweidler law follows from (16) as the description of the large frequency wing of the α-spectrum. It describes the dynamics on the interval $t_\sigma \ll t \ll t'_\sigma$. The exponent b is the same for all correlators measured at the same transition. But exponent b is not universal, different systems may exhibit different values for b. It is plausible (Götze and Sjögren 1987a) and supported by numerical solutions of (17) that there is no low frequency anomaly of the α- relaxation master function. With some reservation because of a lacking mathematical proof, one concludes that there is no stretching anomaly on the low frequency wing of the α-peaks. Unless there is some specialty, one gets a bump for the α-spectrum, which is asymmetrically stretched by the von Schweidler process. The latter is the essence of the stretching phenomenon. Let us emphasize that the fractal exponents in (2) and (16) have been obtained as general implications of the dynamics, connected with the bifurcation as described by the elementary equation (10). No fractals have been assumed or built into the basic equations of the MCT. In particular, no fractals have been assumed or obtained for variations in configuration space.

3.3. Double peak phenomena

3.3.1. Crossing singularities. The bifurcation hypersurface $\mathcal{H}$, mentioned above in connection with (10) and (11) consists of several smooth pieces. The inner points of these pieces are Whitney fold bifurcation singularities, as is obvious from (12). Two such pieces may be joint on $(N-2)$-dimensional sets $\mathcal{H}'$ of Whitney cusp bifurcation singularities. Two pieces may intersect forming $(N-2)$-dimensional sets $\mathcal{H}_K$ of crossing points (Götze and Haussmann 1988). Inherently cusp points do not have liquid states $V \in D_L$ in their neighborhood. Figure 6 illustrates the various possibilities by a two-dimensional cut through the parameter space $\mathcal{K}$. The $v_0 - v_1$ parameter plane is shown to cut three pieces of $\mathcal{H}$ in lines. A full line, denoted by (2), is joint by some other line, shown as a chain curve, in a cusp; the latter is marked by a circle. A third line denoted by (1) and shown partly as a full line and partly dotted, crosses the line (2).

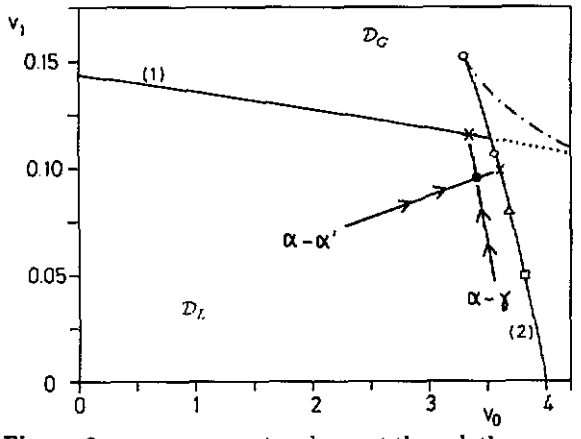

Figure 6. $v_0 - v_1$ parameter plane cut through the parameter space $\mathcal{K}$. See text for details.

The two surface pieces, which form a corner, enter the dynamical theory asymmetrically: on one surface say $\mathcal{H}^{(1)}$, all glass form factors $f_q^{(1)}$ are smaller than the corresponding ones $f_q^{(2)}$ on the other surface, say $\mathcal{H}^{(2)}$ (Götze 1991).

$$f_q^{(1)}(V_K) < f_q^{(2)}(V_K) \qquad q = 1, \ldots, M,\ V_K \in \mathcal{H}_K. \tag{21}$$

The continuation of $\mathcal{H}^{(1)}$ through $\mathcal{H}^{(2)}$, indicated in dots in figure 6, does not belong to the set D_c of glass transition singularities. The bifurcation points of (10), which occur on this part of $\mathcal{H}^{(1)}$, have no relevance for the glass form factor $f_q(V)$, as it occurs for the correlators in the long time limit.

Generically the path $V(T)$ does not hit the corner V_K. But it may come close to V_K, as indicates by the dot in figure 6. In that case the slow dynamics will reflect the glass transition precursor as caused by the two possible transitions. The tendency for arrest at $f_q^{(2)}$ governs the first process for times exceeding $t_0(V_K)$. It is ruled by the exponent parameter $\lambda^{(2)}(V_K)$ and the exponent $a^{(2)}, b^{(2)}$ for $\mathcal{H}^{(2)}$. $\Phi_q(t)$ approach $f_q^{(2)}$ as critical decay $f_q^{(2)} + h_q^{(2)}/t^{a^{(2)}}$. It performs the α- process for $\mathcal{H}^{(2)}$ which is started with the corresponding von Schweidler law $\Phi_q(t) - f_q^{(2)} \propto -t^{b^{(2)}}$. This α-process produces susceptibility peaks at some $\omega_\alpha^{(2)}$. For longer times the system is close to an arrest at $f_q^{(1)}$. The corresponding dynamics is characterized by the exponent parameter $\lambda^{(1)}(V_K)$ and the connected exponents $a^{(1)}, b^{(1)}$. The β-process is introduced by the critical decay towards $f_q^{(1)}$, which then crosses over to the von Schweidler behaviour for $\mathcal{H}^{(1)}$: $\Phi_q(t) - f_q^{(1)} \propto -t^{b^{(1)}}$. Susceptibility peaks are formed at some $\omega_\alpha^{(1)}$, which correspond to the α-process of $\mathcal{H}^{(1)}$. Therefore a two peak pattern is created. One peak at $\omega_\alpha^{(2)}$ has area $f^{(2)} - f^{(1)}$. It is accompanied by another peak at some lower frequency $\omega_\alpha^{(1)} < \omega_\alpha^{(2)}$, which has area $f^{(1)}$. The closer V is to the corner V_K, the more the peaks are separated. Both peaks are connected with the full α–β-relaxation pattern of the respective transitions. The relative size of the two peaks depends on the details of the model.

There are two relevant control parameters, which govern the sensitive variations of the spectra due to the changes of physical parameters like the temperature. These are the two separation parameters $\sigma_1(V)$ and $\sigma_2(V)$, characterizing the two pieces $\mathcal{H}^{(1)}$ and $\mathcal{H}^{(2)}$. There are two generic possibilities for a liquid to glass crossover near a corner. Either $V \to V_c \in \mathcal{H}^{(2)}$. In this case $\sigma_2 \to 0$ for $T \to T_c$, while the other parameter approaches some constant $\sigma_1(V) \to \sigma_1(V_c^{(2)}) =: X^{(1)} < 0$. Or $V \to V_c \in \mathcal{H}^{(1)}$. In this case $\sigma_1 \to 0$ for $T \to T_c$ and the other separation parameter tends to some constant $\sigma_2(V) \to \sigma_2(V_c) =: X^{(2)} < 0$. The asymptotic variation of the double peak pattern for $T \to T_c$ is quite different for the two scenarios.

3.3.2. The α'–α-scenario. Let us consider the transition through $\mathcal{H}^{(2)}$ on a path similar to the one indicated in figure 6 by a line marked α–α'. For $T \to T_c$ the longest timescale is the α-relaxation scale $\omega_\alpha^{(2)}$ for the transition at $V_c \in \mathcal{H}^{(2)}$. It diverges for $T \to T_c$, while the scales connected with σ_1 remain finite. The whole double peak pattern obeys the time temperature superposition principle in the leading asymptotic expansion. The solution of the scaling equation (17) and (18) yields the two peak master function; *it does not contain the β-relaxation part of the transition* through $\mathcal{H}^{(2)}$. Its large frequency asymptote is the von Schweidler law with exponent $b^{(2)}$. The low frequency peaks exhibit the full α–β pattern of the transition through

$\mathcal{H}^{(1)}$, as it is determined by the separation parameter $X^{(1)}$. It depends sensitively on $X^{(1)}$; in particular the α'-peak moves down in frequency if $X^{(1)}$ is lowered. This is illustrated in figure 7. The α-scaling law holds only in that limit, where temperature dependence of $X^{(1)}$ can be neglected. This is the case only for very small $(T - T_c)$. Therefore one gets stronger deviations from the time temperature superposition principle for the double peak scenario, then one usually gets for transitions away from crossing singularities V_K. Obviously these findings qualitatively explain the experiments, discussed in connection with figures 4 and 5.

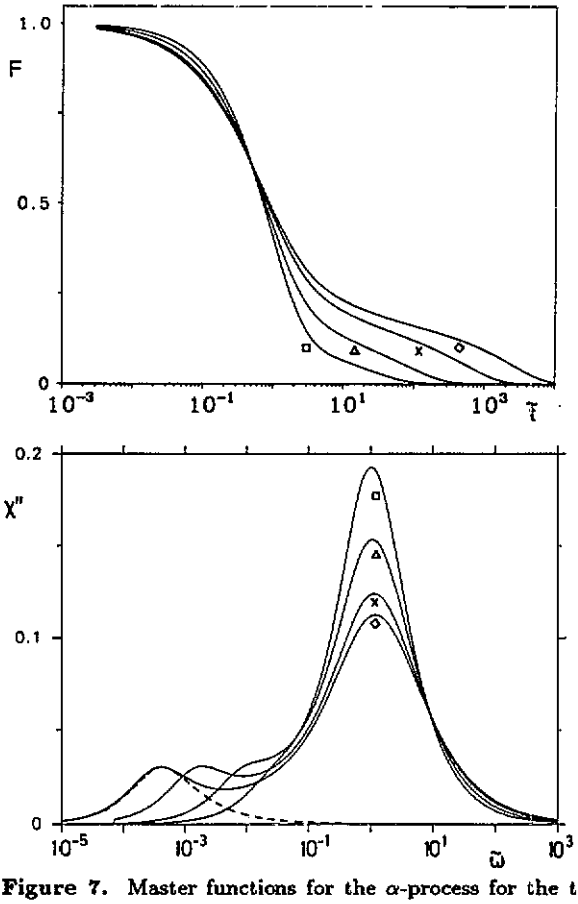

Figure 7. Master functions for the α-process for the transition points noted in figure 6. The broken curve is a shifted master function for a transition through $\mathcal{H}^{(1)}$ calculated at the point marked by a star in figure 6; see text.

3.3.3. The γ-peaks. The evolution of the low frequency spectra upon approaching $\mathcal{H}^{(1)}$ can be inferred from the preceding discussion. A possible path is indicated in figure 6 by a line marked α–γ. For small $X^{(2)}$ one gets double peak patterns described by master functions calculated from $V_c \in \mathcal{H}^{(2)}$. However, only the scale of the low frequency peak connected to σ_1 varies critically. The sequence of spectra shown in figure 7 describes such a scenario where the α-peak connected with $\mathcal{H}^{(2)}$ appears as a specialty of the high frequency dynamics. For the mathematical discussion of the transition, the upper peak is treated as a transient dynamics, where the time scale

is short and smoothly varying compared to the scales ruling the transition. Solving the scaling equation (17) and (18) at $V_c \in \mathcal{H}^{(1)}$, eliminates the β-contribution of this transition and the spectrum above it. It yields the α-relaxation part of the $\mathcal{H}^{(1)}$-transition only. This is illustrated by the broken curve in figure 7. It shows a shifted master spectrum, calculated at the point on $\mathcal{H}^{(1)}$ which is marked by a star in the phase diagram of figure 6. For small σ_1 the α-relaxation scales onto this master function.

The spectral peak above the glass transition spectrum is different in three aspects from what one expects for some molecular resonance. Its position is located far below what is typical for microscopic transient dynamics, the position is rather sensitive to control parameter variations and the peak is stretched. The upper peak is different from a typical α-resonance since it exhibits stretching and fractal behaviour not only on the high frequency part but also on the low frequency one. The stretching on the upper part is caused by the von Schweidler law with exponent $b^{(2)}$. The stretching on the lower part is due to the critical spectrum of the transition through $\mathcal{H}^{(1)}$. The corresponding exponent is $a^{(1)}$. This may lead to rather symmetrical peaks as shown, accidentally, in figure 7. The upper peak is also different from a standard β-resonance. The latter are typically much broader and their intensity is smaller than the upper resonance shown in figure 7. All these findings support the conclusion that the found scenario is the relevant one for the pattern of an α-resonance which is accompanied by a high frequency γ-peak (McCrum *et al* 1967).

The essence of the preceding discussion is the following: near a corner a double peak structure of the susceptibility spectrum is found. Whether this is interpreted as α–α'-or α–γ-pair depends on the variation of the spectrum as a function of temperature.

3.3.4. Triple peak scenarios. Obviously, the preceding discussion can be generalized. The next, more complicated, case deals with a corner V_K, where three hypersurface pieces, say $\mathcal{H}^{(1)}, \mathcal{H}^{(2)}$ and $\mathcal{H}^{(3)}$ meet. The surfaces are put in a sequence, generalizing (21)

$$f_q^{(1)}(V_K) < f_q^{(2)}(V_K) < f_q^{(3)}(V_K) \qquad q = 1, \ldots, M. \tag{22}$$

There appear three α-peaks of frequencies $\omega_\alpha^{(1)} < \omega_\alpha^{(2)} < \omega_\alpha^{(3)}$ with areas $f_q^{(1)}$, $f_q^{(2)} - f_q^{(1)}$ and $f_q^{(3)} - f_q^{(2)}$ respectively. There are three scenarios for a liquid to glass crossover. If $\mathcal{H}^{(3)}$ is crossed, the whole three-peak pattern obeys the time temperature superposition principle. Such a scenario was observed recently for a system of PPG with lithium ions as solute (Fu *et al* 1991). If $\mathcal{H}^{(2)}$ is crossed, there will be a double peak pattern, which scales as discussed in connection with figures 4 and 5. Above this pattern there is a γ-resonance. If $\mathcal{H}^{(1)}$ is crossed, there will be a normal relaxation pattern for a liquid to glass crossover, consisting of the temperature or concentration dependent α- and β-spectrum. Above those spectra are two stretched resonances, a γ-peak and a δ-peak.

3.4. Solution of the scaling equation

A previously used iteration procedure for the numerical evaluation of the master functions $F_q(t)$ required one Laplace transform and one back transform in every iteration step (Götze and Sjögren 1987a). This procedure is not practical in the present context,

since Laplace transforms are very cumbersome for functions, which are structured and stretched on such large windows as shown in figure 5. Therefore an iteration procedure for the solution of (17) and (18) will be used, which exploits the causality properties of the MCT: the functions $F_q(t)$ are determined by the correlators $F_k(t')$ where t' precedes t. At the end of the procedures Laplace transforms $F_q(z)$ of the correlators and $m_q(z)$ of the kernel (18) are calculated, $z = \omega + \imath 0$. The correlators yield the susceptibility $\chi'(\omega) + \imath\chi''(\omega)$. The kernels are used as a global check for accuracy, by verifying the Laplace transformed version of (17) and (18).

$$F_q(z) = -1/[z - 1/m_q(z)]. \tag{23}$$

The functions $F(t)$ and $m(t)$ vary more slowly for large times than for small ones. To separate slow and fast variations in the convolution integral in (17), one writes with $\tau = t/2$:

$$\begin{aligned} I &= \frac{\mathrm{d}}{\mathrm{d}t}\int_0^t m(t-t')F(t')\,\mathrm{d}t' \\ &= F(\tau)m(\tau) + \int_0^\tau \dot{m}(t-t')F(t')\,\mathrm{d}t' + \int_0^\tau \dot{F}(t-t')m(t')\,\mathrm{d}t'. \end{aligned} \tag{24}$$

Let us consider the following integral extended over $t_1 < t < t_2$:

$$I = \int \dot{A}(t-t')B(t')\,\mathrm{d}t'. \tag{25}$$

It can be written as

$$I = [A(t-t_1) - A(t-t_2)](t_2-t_1)^{-1}\int B(t')\,\mathrm{d}t' + O. \tag{26}$$

The first term is of order $h = (t_2 - t_1)$ while the second one,

$$O = \int \{[\dot{A}(t-t') - (A(t-t_1) - A(t-t_2))/h][B(t') - \frac{1}{h}\int \mathrm{d}t''B(t'')]\}\,\mathrm{d}t' \tag{27}$$

is of order h^3. The approximation consists of dropping O for the evaluation of I. This will be done for the evaluation of I on a grid of stepsize h. With $t_i = ih, t = t_n, \tau = n_2 = n/2, F_i = F(t_i), m_i = m(t_i)$ and

$$\mathrm{d}F_i = \int_{t_{i-1}}^{t_i} F(t')\,\mathrm{d}t'/h \qquad \mathrm{d}M_i = \int_{t_{i-1}}^{t_i} m(t')\,\mathrm{d}t'/h \tag{28}$$

one gets the approximation

$$I = m_{n_2}F_{n_2} + \sum_{i=1}^{n_2}[\mathrm{d}F_i(m_{n-i+1} - m_{n-i}) + \mathrm{d}M_i(F_{n-i+1} - F_{n-i})]. \tag{29}$$

The discretized version of the scaling equation reads:

$$F_n(1 + \mathrm{d}M_1) = m_n(1 - \mathrm{d}F_1) + C_n \tag{30}$$

$$\begin{aligned} C_n = &-m_{n_2}F_{n_2} + \mathrm{d}F_1 m_{n-1} + \mathrm{d}m_1 F_{n-1} \\ &+ \sum_{i=2}^{n_2}[\mathrm{d}F_i(m_{n-i} - m_{n-i+1}) + \mathrm{d}M_i(F_{n-i} - F_{n-i+1}] \end{aligned} \tag{31}$$

$$m_i = \mathcal{F}(V_c, F_i). \tag{32}$$

Here and in the following the index q is dropped for simplification of the notation. C_n is given by F_i for $i = 2,\ldots,n-1$ and by $\mathrm{d}F_i$, $\mathrm{d}M_i$ for $i = 1,\ldots,n_2$. Knowing the latter for $i = 1,\ldots,N_2$ one can solve the equations recursively to get F_i, m_i for $i = N_2+1,\ldots,2N_2$.

The solution of (30) for F_n, m_n is elementary only for very special cases . In general another iteration is used:

$$F_n^{(k+1)}(1+\mathrm{d}M_1) = m_n^{(k)}(1-\mathrm{d}F_1) + C_n \tag{33}$$

$$m_n^{(k)} = \mathcal{F}(V_c, F_n^{(k)}). \tag{34}$$

One can show that $F_n^{(k)} > F_n^{(k+1)} \geqslant 0$. Therefore the limit $F_n^{(k)} \to F_n$ exists. The proof implies also $F_n > F_{n+1} \geqslant 0$ (Hofacker 1990).

Having extended the solution with step size h from $(N/2)$ points to N points, a decimation is carried out. One transforms: $h \to 2h, F_{2i} \to F_i$, $\mathrm{d}F_i \to \mathrm{d}F_i^{\mathrm{new}}$, $\mathrm{d}M_i \to \mathrm{d}M_i^{\mathrm{new}}$. Here

$$\mathrm{d}F_i^{\mathrm{new}} = (\mathrm{d}F_{2i} + \mathrm{d}F_{2i+1})/2 \qquad i \leqslant N/4 \tag{35}$$

$$\mathrm{d}F_i^{\mathrm{new}} = (F_{2i} + 4F_{2i-1} + F_{2i-2})/6 \qquad i > N/4 \tag{36}$$

and corresponding formulae hold for $\mathrm{d}M_i^{\mathrm{new}}$. The whole procedure is started with $N/2$ points, which are calculated from the short time expansions, discussed above in connection with (16).

The results to be shown below are evaluated typically with $N = 600$. In the first step either (16) or extension by one more term are used. The achieved relative accuracy was better than 10^{-5}. The calculation were done on an IBM-AT. For the $M = 1$ models two minutes calculation time were used per decade. The computation time is of the order $O(NM^2, N^2M)$.

4. Examples for mode coupling theory results

Simple MCT models deal with a single correlator: $M = 1$. In this case the mode coupling functional is a polynomial of degree N : $\mathcal{F}(f) = v_1 f + v_2 f^2 + \ldots + v_N f^N$. The vector in control parameter space combines the coefficients $V = (v_1,\ldots,v_N)$. If one specializes further to a monomial like $\mathcal{F}(f) = v_2 f^2$ (Leutheusser 1984, Bengtzelius *et al* 1984), the scaling equation (17) and (18) is solved readily, albeit by a Debye function: $F(\tilde{t}) = f_c \exp(-\tilde{t})$. These models are the only ones, where the α-process is described as stochastic relaxation. These non-generic specializations miss the essential feature of glassy dynamics, viz., the stretching. The most simple meaningful model uses a two-dimensional control parameter space by specializing (Götze 1984).

$$\mathcal{F}(f) = v_1 f + v_2 f^2. \tag{37}$$

The master functions in this case are very close to the Kohlrausch results (DeRaedt and Götze 1986, Götze and Sjögren 1987a). This is demonstrated in figure 8 for a representative example. The master functions follow (1) for a large dynamical range. More than the upper 98% of the α-peak is determined accurately by the stretched exponential decay. The von Schweidler law is valid only for very large frequencies

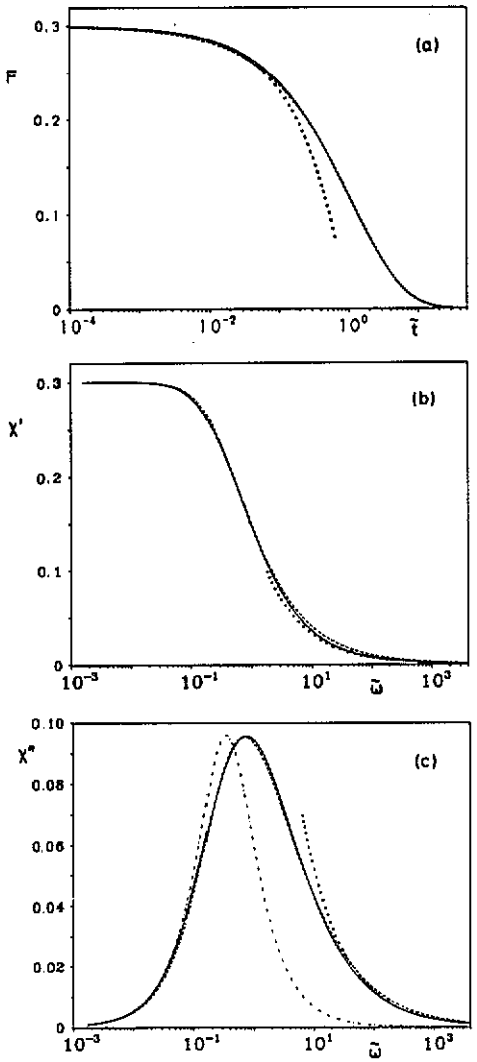

Figure 8. Master function $F(\tilde{t})$, reactive part of the susceptibility $\chi'(\tilde{\omega})$ and susceptibility spectrum $\chi''(\tilde{\omega})$ for the model (37) ; $\lambda = 0.7$, $f^c = 0.3$, $v_1 = 0.816$, $v_2 = 2.041$. The broken curves are Kohlrausch functions with exponent $\beta = 0.59$. The dotted curves are the von Schweidler asymptotes with exponent $b = 0.64$. The chain curve in (c) is a Debye resonance, shifted so as to fit the low frequency part of $\chi''(\tilde{\omega})$.

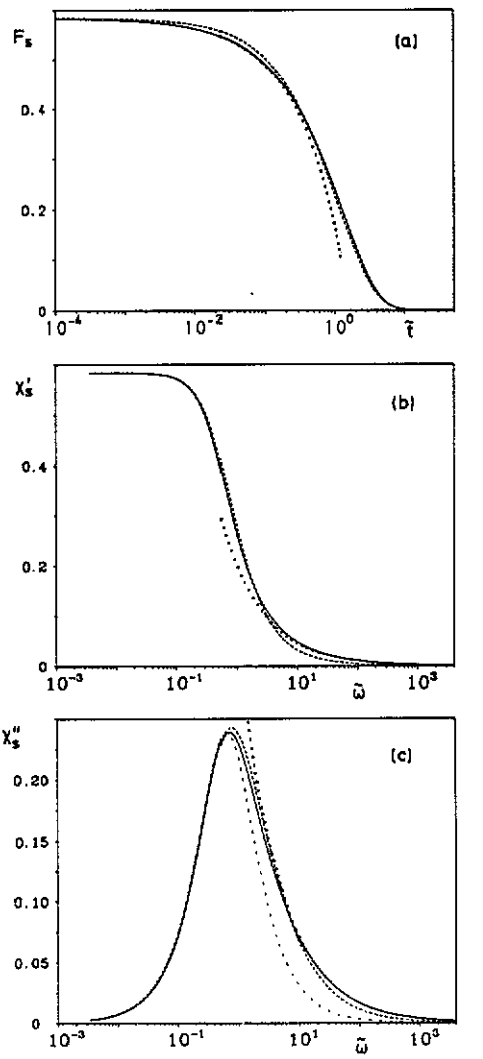

Figure 9. Master functions for the second correlator of the two component model (38) for $v_s = 8$. The results for the first correlator are shown in figure 8. The broken curves are Kohlrausch functions with exponent $\beta = 0.80$. The dotted curves are the von Schweidler asymptotes for exponent $b = 0.64$. The chain curve in (c) is a Debye resonance.

$\log\tilde{\omega} > 1.5$. It describes only that part of the high frequency α-peak wing, where $\chi''(\omega)/\chi''_{\max} < 0.2$. Only the first 10% of the decay of $F(\tilde{t})$ follows (2) in this case.

The simplest two component model leaves the equation of motion of one correlator, say $\Phi(t)$ with α-relaxation master function $F(\tilde{t})$, unchanged. The mode coupling

functional of the second correlator, say $\Phi_s(t)$, with α-relaxation master function $F_s(\tilde{t})$, is governed by the simplest polynomial (Sjögren 1986)

$$\mathcal{F}_s = v_s f f_s. \tag{38}$$

Figure 9 exhibits the master functions for $v_s = 8$, using the results of figure 8 as input for f. The susceptibility spectrum χ_s'' for large frequencies is above the one produced by the best Kohlrausch fit. The von Schweidler law has a large range of validity. It accounts well for the high frequency α-peak tail, where $\chi''(\omega)/\chi''_{\max} < 0.5$. Formula (2) describes 20% of the initial decay of $F_s(\tilde{t})$. The spectrum $\chi''(\omega)$ in figure 9 shows the qualitative features discussed above in connection with figures 1-3. A quantitative fit of the quoted data is not possible by the model (38). The resonance for χ_s'' is too narrow and the Debye law describes the low frequency part of the spectrum too well in comparison to what is shown in figures 1-3.

The simplest relevant model, specializing the quadratic mode-coupling functional (9), deals with two correlators and uses for $q = 0, 1$ the following formulae (Krieger and Bosse 1987)

$$\mathcal{F}_0(f_0, f_1) = v_0 f_0^2 + v_1 f_1^2 \qquad \mathcal{F}_1(f_0, f_1) = v_s f_0 f_1. \tag{39}$$

The control parameter space has three dimensions: $V = (v_0, v_1, v_s)$. This model exhibits the line crossing phenomenon (Götze and Haussmann 1988). The phase diagram in figure 6 was evaluated for this model for the cut through K with $v_s = 50$. At the shown crossing point one gets for the two exponent parameters $\lambda^{(1)} = 0.63, \lambda^{(2)} = 0.67$ and the form factors have the values: $f_0^{(1)} = 0.070$, $f_1^{(1)} = 0.714$, $f_0^{(2)} = 0.423$, $f_1^{(2)} = 0.953$. The master functions shown in figure 7 refer to this model where the parameter points are indicated by the various symbols in figure 6. The α-peaks for model (39) and also the main peak of the double peak pattern, have a signature similar to that shown in figure 9.

Schematic models of the kind listed above have been invented to demonstrate with a minimum of mathematical effort some generic features of the MCT. Such models imply also additional results like deviations from asymptotic scaling laws. Those results are not necessarily representative for the full theory as specified by (9). Examples for such artifacts of schematic models are the connection $f_c = 1 - \lambda$, which follows from (37), or the narrowness of the χ_s''-peak in the model (38). It should be of no surprise, that none of the so far studied schematic models can account quantitatively for the data quoted in figures 1–5. It seems of some interest to know, however, which effort has to be made within the mathematical theory in order to fit relevant data quantitatively. This is the motivation to consider an $M = 3$ model. The mode coupling functional (9) for three correlators, labelled by $q = 0, 1, 2$, shall be specialized as follows:

$$\mathcal{F}_0(f_0, f_1, f_2) = v_0 f_0^2 + v_1 f_1^2 + v_2 f_2^2 \tag{40}$$

$$\mathcal{F}_i(f_0, f_1, f_2) = v_{si} f_0 f_i \qquad i = 1, 2. \tag{41}$$

In this case the dimensionality of $\mathcal{K}$ is five: $V = (v_0, v_1, v_2, v_{s1}, v_{s2})$. The model (39) is obtained as limit for $v_2 = 0$. Previously invented tricks (Götze and Haussmann 1988) can be used to calculate simply the bifurcation hypersurface $\mathcal{H}$, the form factors at

the transitions f_q^c, the critical amplitudes h_q and also the expression for the exponent parameter:

$$\lambda = \frac{(1-f_0)^3\left[v_0 + (3/f_0^4)(v_1/v_{s1}^2 + v_2/v_{s2}^2)\right]}{1 + 2\left((1-f_0)/f_0\right)^3(v_1/v_{s1} + v_2/v_{s2})} \tag{42}$$

Crossing singularities occur if v_{s1} or v_{s2} exceed $v_c = 24.78$.

Data fits with (40) and (41) have been performed using the correlator for $q = 0$. Fits were started by reading off the von Schweidler exponent b according to (2) from a $\log\chi''$ versus $\log\omega$ diagram for the data. This information restricts $\boldsymbol{V}$ to a three-dimensional subset of the transition hypersurface. As a second step, the large frequency part of the α-peak was fitted with $v_{2s} = v_2 = 0$. Then v_2 was switched on to improve the agreement between fit and data.

The full curves in figures 1–3 show results for (40) and (41). The fit for the CKN-data in figure 1 was made for the absorptive part of the modulus $M''(\omega)$. Comparison of the theoretical results for $M'(\omega)$ with the data for the reactive part demonstrates the consistency of the procedure. The parameter values used are $\lambda = 0.82\,(b = 0.44)$, $v_0 = 2.88$, $v_1 = 0.195$, $v_2 = 0.032$, $v_{s1} = 20$, $v_{s2} = 45$. The fit for the PVA spectrum in figure 3 was done with the same exponent parameter λ, using $v_0 = 2.81$, $v_1 = 0.212$, $v_2 = 0.04$, $v_{s1} = 17$, $v_{s2} = 45$. The fit for OT in figure 2 refers to the values $\lambda = 0.84\,(b = 0.41), v_0 = 2.86$, $v_1 = 0.174$, $v_2 = 0.08$, $v_{s1} = 15.2$, $v_{s2} = 30$.

The full curve in figure 4 was calculated for $v_0 = 2.89$, $v_1 = 0.193$, $v_2 = 0.041$, $v_{s1} = 17$, $v_{s2} = 144$. This yields $\lambda = 0.86$, i.e. $b = 0.375$. In figure 10 the three correlators $F_q(\tilde{t})$ and susceptibility spectra χ_q'' are shown. The PPG data of Fu *et al* (1991) can be fitted reasonably with parameters close to those chosen for the data of Johari (1986). The full curves in figure 10 are calculated for $v_0 = 2.93$, $v_1 = 0.191$, $v_2 = 0.0355$, $v_{s1} = 18$, $v_{s2} = 161$. This corresponds to an exponent parameter $\lambda = 0.87$ implying a von Schweidler exponent $b = 0.357$. In order not to overload the figure, only the data for two temperatures are reproduced. One notices that the high frequency data in figure 11 deviate somewhat from the von Schweidler asymptote. This effect would show up more drastically if data for lower temperatures were included in the figure, thereby extending the dynamical window for the rescaled frequency. A possible reason might be phonon assisted hopping transport. This relaxation mechanism is not included in the theory for the idealized transition studied in this paper.

The MCT predicts a relation between the anomalous dimensionality b of the spectrum and the exponent γ, ruling the α-relaxation scale. This was discussed above in connection with (13). The mentioned value of b for PPG yields $\gamma = 3.54$. A $\omega_m^{1/\gamma}$ versus T plot, with $\omega_m = \omega_\alpha$ denoting the maximum peak position, should give a straight line, which intersects the abscissa for $T = T_c$. Figure 12 shows indeed, that the power law variation for t_σ' is observed for the large temperature interval 260 K $< T <$ 360 K. The power law prediction for the α-relaxation scale and the connection between the two exponents b and γ describes properly the shift of the resonance by a factor 500. The critical temperature is estimated as $T_c = 237$ K. This estimate has to be taken with reservation. Since T_c is a crossover temperature from liquid to glass dynamics, a reliable estimate should be based on a quantitative analysis of data measured above as well as below T_c.

The MCT for the idealized liquid to glass transition becomes partly irrelevant for experiments referring to temperatures at or below T_c. This is obvious from figure 12.

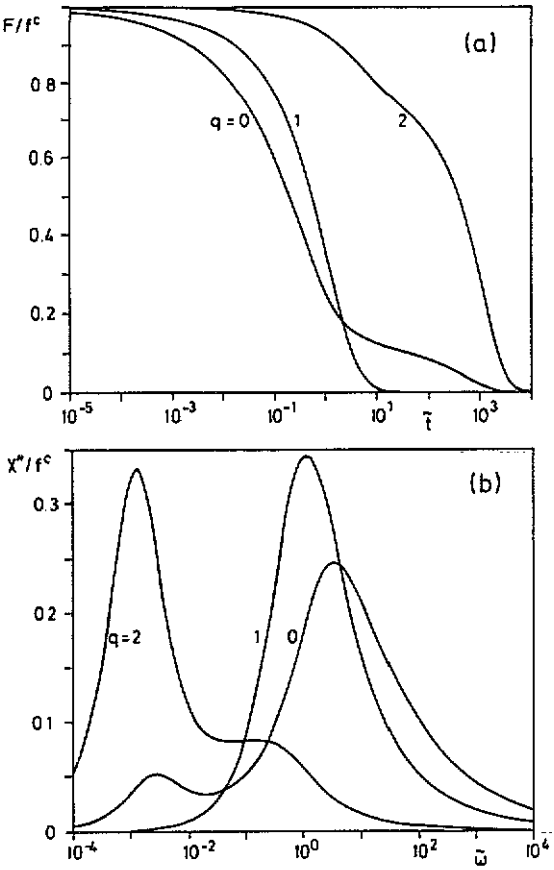

Figure 10. Normalized master functions F_q/f_q and spectra χ_q''/f_q for model (40), (41). The parameters are specified in the text. The form factors are $f_0^c = 0.206$, $f_1^c = 0.715$, $f_2^c = 0.966$. χ_0'' is the spectrum shown also in figure 4.

The frequency ω_m does not vanish for $\sigma \propto T_c - T \to 0$ according to (13), rather it crosses over to some different law for $T < T_c$. Phonon assisted transport is the physical mechanism, which prevents the idealized arrest for $T < T_c$. The equations for the α-peak shapes, which include the mentioned processes, have not been studied in sufficient detail yet. It is known that the simple scaling law (5) may become invalid for $T < T_c$. The von Schweidler law (2) describes the high frequency α-process also for $T < T_c$ albeit with a temperature dependent exponent b (Götze and Sjögren 1987b,1988). The MCT has not yet produced a handy formula to describe the α-relaxation scale ω_m for $T \approx T_c$. It is well known, that the Vogel–Fulcher formula fits relaxation scale variations over many decades properly. This is the case also for the PPG data under discussion; $\omega_m \propto \exp(-985/((T/K) - 171))$ accounts for the experiments of Fu *et al* (1991) perfectly. The MCT results for the α-peak shapes, discussed in this paper, can be used only, if phonon assisted hopping effects do not influence the master functions strongly. This is the case, if the time temperature superposition principle is valid. Then one can extrapolate the data into the region $T > T_c$, where the theory for the idealized transition is proposed to apply.

The 3-component model (40) and (41) is also the simplest example producing a

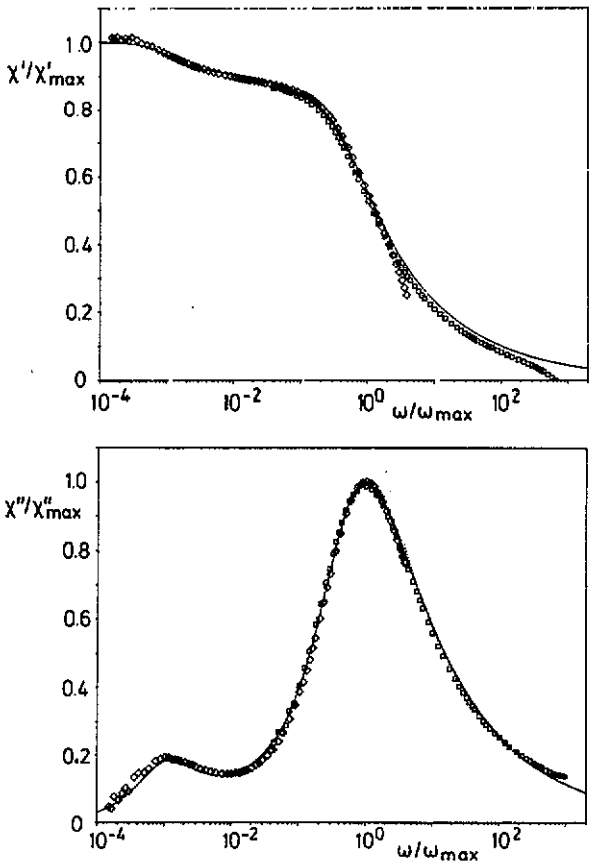

Figure 11. Normalized results for reactive and absorptive parts of the dielectric function of PPG as measured by Fu (1990) and Fu et al (1991) for $T = 227.4$ K, $\omega_{max} = 13.5$ Hz (squares) and $T = 253.6$ K, $\omega_{max} = 3280$ Hz (diamonds). The full curves are MCT results for model (40) and (41) with parameters explained in the text. The dotted curve is a von Schweidler asymptote for exponent $b = 0.36$.

triple peak. Figure 13 shows a spectrum for parameters chosen close to a three surface corner: $v_0 = 3.37$, $v_1 = 0.086$, $v_2 = 0.063$, $v_{s1} = 22$, $v_{s2} = 88$.

Finally we want to re-emphasize that the number of peaks in the spectrum is a consequence of the topology of the bifurcation hypersurface $\mathcal{H}$. In order to obtain an n-peak spectrum, the dimensionality N of the control parameter space $\mathcal{K}$ must not be smaller than n. The number M of correlators is not essential. For example a one component model with $\mathcal{F}(f) = v_2 f^2 + v_N f^N$ can produce a double peak provided $N \geqslant 10$.

5. Conclusions

The α-process is a general feature of glassy dynamics observed in a variety of substances ranging from the molten salt CKN to polymers with large molecular weights. Therefore it seems desirable to interpret this phenomenon in a general way, that transcends the details of the molecular structure and does not require specific models for

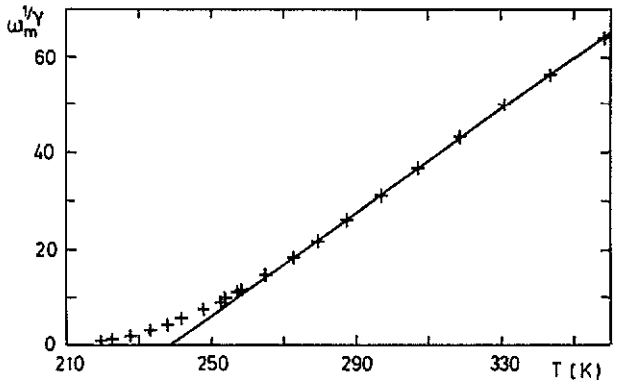

Figure 12. $\omega_m^{1/\gamma}$ versus temperature for the data measured by Fu (1990) and Fu *et al* (1991) for PPG. ω_m is the α-peak position in Hz. $\gamma = 3.54$. The straight line is a guide for the eye.

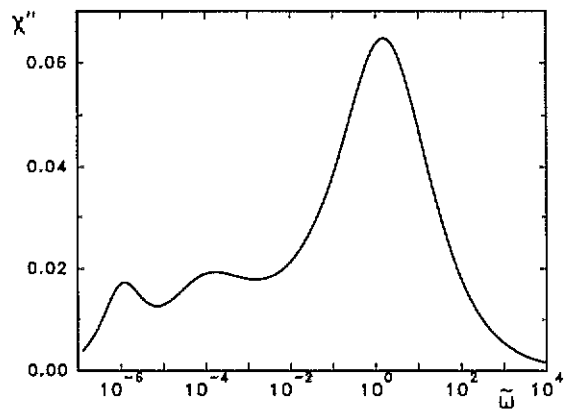

Figure 13. Susceptibility spectrum of the 3 component model (40) and (41) with parameters specified in the text.

the microscopic details (Johari 1986). The MCT for the idealized liquid to glass transition is such a general approach. It is based on transparent equations of motion for a set of correlation functions which characterize the dynamics in a statistical manner. These equations are completely regular; the essence is a mode coupling functional, which is a polynomial of the correlators. But the equations are non-linear. There appear various bifurcation singularities; the simplest one describes a transition from liquid behaviour to ideal glass dynamics. The singularities cause subtle anomalies for the long time dynamics. The novel results for the dynamics are due to the retardation effects. The qualitative features of the singularities reflect the topology of the bifurcation hypersurface. Therefore the results are stable with regard to modifications of the theory; they can be understood qualitatively and, to a large extent, even quantitatively by analytic calculations. In this paper it was shown, that the MCT picture for the α-process exhibits the same subtleties as the experiments.

Within the MCT the von Schweidler law appears as the reason for the generally observed stretching of the α-process. It describes the dynamics for times which are short compared to the relaxation time τ of the α-process, but long compared to the

time scale for the β-dynamics. It accounts for the high frequency wing $\omega\tau \gg 1$ of the α-peaks. No stretching anomaly appears in the theory nor in the experiments on the low frequency wing $\omega\tau \ll 1$ of simple α-resonances. The Kohlrausch fit accounts well for the spectra for $\omega\tau \ll 1$ for trivial reasons. It describes properly the upper half of the resonances, since it implies also a crossover to power law spectra for $\omega\tau \gg 1$. Occasionally the Kohlrausch fit accounts for the major part of the α-resonance. Also the most simple example for the MCT exhibits this result as shown in figure 8. In this case, the von Schweidler law holds only for very large frequencies, so that it can hardly be identified in the spectra.

Kohlrausch fits are usually optimized for the upper part of the α- resonance. The exponent β in the stretched exponential law is in one to one correspondence to the peak half width. As a typical result one finds in the MCT as well as in experiments, that the Kohlrausch fit fails in the high frequency wing where $\chi''/\chi_{max} < 0.2$. This occurs in particular in those cases where corrections to the von Schweidler asymptote are so small that (2) accounts for the whole region $\omega/\omega_{max} \gg 1$. The range of validity of the von Schweidler law is different for different correlation functions measured for the same transition. For that reason also, the Kohlrausch exponent β may be different for different spectra referring to the same system. Within the MCT the Kohlrausch exponent β is a mere fit parameter without any mathematical or physical significance. The anomalous dimensionality b of the von Schweidler process appears, on the other hand, as a critical parameter specifying the dynamics. It is the same for all correlators of the given system. But different systems exhibit different exponents b.

The inadequacy of the Kohlrausch fit for α-peaks of dielectric loss spectra was recently demonstrated for a variety of organic glass formers by Dixon *et al* (1990). For most of the systems they studied also strong violations of the time temperature superposition principle were detected. The peak half width increased with decreasing temperature. However, the authors discovered a new scaling relation, allowing them to describe all their spectra from one single master function. The new feature of their master function is the behaviour of the high frequency tails. This is deduced from data where the α-peak position is in the low frequency band. These data refer presumably to a region $T \ll T_c$. For $T < T_c$ the MCT also predicts violations of the simple α-scaling. But since the α-peak equations for $T < T_c$ (Götze and Sjögren 1987b) could not yet be solved it is unclear whether the MCT can reproduce the important discoveries of Dixon *et al* (1990).

Double peak relaxation patterns are a generic implication of the MCT. They are caused by corners of the boundary between liquid and glass states. Even simple specializations of the MCT equations show this phenomenon, since even simple models exhibit the topological feature of the crossing of bifurcation hypersurface pieces. There are two possibilities for liquid to glass crossovers near such crossing singularities. One explains the α'–α-double peak and the other causes the pattern of an α–γ-peak pair. There may also be corners, where three pieces of the bifurcation hypersurface intersect. Generically, a system may come close to such corner. In case there are three stretched susceptibility peaks leading e.g. to the α–γ–δ-peak scenario. A double peak susceptibility spectrum is equivalent to a double step behaviour of the reactive response $\chi'(\omega)$, as shown in figure 11. The size of the two steps $\Delta\chi$ due to the α'- and the α-peak respectively is given by the areas of the respective spectral peaks. Suppose, one measures $\chi'(\omega_0)$ for a fixed test frequency ω_0 as function of temperature. One gets a step $\Delta\chi'$ at a temperature T_g', when $\omega_\alpha'(T_g') = \omega_0$. A second step occurs at a temperature $T_g < T_g'$, if $\omega_\alpha(T_g) = \omega_0$. These steps describe the transformation of

the supercooled liquid into the glass state in a conventional quenching experiment. A simple α-peak describes this transformation as an one step process at T_g, while the double peak scenario is connected to a two step transformation. The conventional transformation temperature refers to the usual scanning speed of 0.3 K/min and this corresponds to $\omega_0 \sim 10^{-3}...10^{-4}s^{-1}$. Many experiments have been identified by Boyer (1985), showing such two step glass transformations; he refers to T_g' as liquid to liquid transition temperature T_{ll}. The double peak phenomenon appears as the natural explanation of those experiments. It seems worthwhile to test this suggestion by spectroscopy. For those examples where the double step was identified in the differential analysis curves for the specific heat, the recently developed heat spectroscopy (Birge and Nagel 1985) might be the appropriate technique.

The shown fits of experiments by the master functions of a simple schematic model demonstrate, that there is no feature in the quoted data which is not properly interpreted by the MCT. However, these fits do not imply a physical understanding of the difference of the dynamics of, say, the anorganic glass former CKN and the polymer PPG. The microscopic differences between various systems enter the vertices $V(q;k,p)$ in (9). These vertices are given by the equilibrium structure of the liquid as reflected by static correlations between pairs and triples of the constituents. Thus, there is the perspective, that the MCT can explain the microscopic origin of the various α-peak shapes. Progress in this direction will depend on whether one can calculate the vertices and understand their properties for realistic systems. So far the vertices and the path of the system in control parameter space $\mathcal{K}$ have been calculated only for simple one component systems of spherical atoms (Bengtzelius *et al* 1984, Bengtzelius 1986) and for simple binary mixtures (Bosse and Thakur 1987, Barrat and Latz 1988). The integration procedure developed in this paper opens the possibility of calculating the α-relaxation master functions for those model systems.

Acknowledgments

We thank cordially Professor H Sillescu for drawing our attention on the double peak phenomenon. Discussions with Professor J R Stevens are gratefully acknowledged; we thank him and his co-workers for the permission to study their data and to show some of their results prior to publication. We thank Dr L Sjögren very much for helpful comments on the manuscript.

References

Adachi K and Kotaka T 1984 *Macromolecules* **17** 120
—— 1985 *Macromolecules* **18** 466
Alper T, Barlow A and Gray R 1976 *Polymer* **17** 665
Barrat J L and Latz A 1990 *J. Phys.: Condens. Matter* **2** 4289
Barrat J L, Roux J N and Hansen J P 1990 *J. Chem. Phys.* **149** 197
Baur M E and Stockmayer W H 1965 *J. Chem. Phys.* **43** 4319
Bengtzelius U 1986 *Phys. Rev.* A **34** 5059
Bengtzelius U, Götze W and Sjölander A 1984 *J. Phys. C: Solid State Phys.* **17** 5915
Beevers M S, Elliot D A and Williams G 1979 *Polymer* **20** 785
Birge N O and Nagel S R *Phys. Rev. Lett.* **54** 2674
Blumen A 1981 *Nuovo Cim.* B **63** 50
Börjesson L, Elmroth M and Torell L M 1990 *Chem. Phys.* **149** 209

Bosse J and Thakur J S 1987 *Phys. Rev. Lett.* **59** 998
Boyer R F 1985 *Polymer Yearbook* ed R A Pethrick (London: Harwood) vol 2, p 233
Brawer S 1985 *Relaxation in Viscous Liquids and Glasses* (Ohio: The American Ceramics Society)
Campbell I A, Flesselles J M, Jullien R and Botet R 1988 *Phys. Rev.* B **37** 3825
Cohen M J and Grest G S 1979 *Phys. Rev.* B **20** 1077
—— 1981 *Phys. Rev.* B **24** 4091
Dixon P K, Wu L and Nagel S R 1990 *Phys. Rev. Lett.* **65** 1108
Ehlich D and Sillescu H 1990 *Macromolecules* **23** 1600
De Dominicis C, Orland H and Lainée F 1985 *J. Physique Lett.* **46** L463
Flesselles J M and Botet R 1989 *J. Phys. A: Math. Gen.* **22** 903
Förster T 1949 *Z. Naturf.* A **4** 321
Frick B, Farago B and Richter D 1990 *Phys. Rev. Lett* **64** 2921
Fu Y 1990 *PhD Thesis* University of Guelph, unpublished
Fu Y, Pathmanathan K, Stevens J R 1991 *J. Chem. Phys.* at press
Fuchs M, Götze W and Latz A 1990 *Chem. Phys.* **149** 185
Götze W 1984 *Z. Phys* B **56** 139
—— 1987 *Amorphous and Liquid Materials* ed E Lüscher, G Fritsch and G Jacucci (Dordrecht: Martinus Nijhoff) p34
—— 1991 *Liquids Freezing and the Glass Transition* ed D Levesque J P Hansen and J Zinn-Justin (New York: Elsevier)
Götze W and Haussmann R 1988 *Z. Phys.* B **72** 403
Götze W and Sjögren L 1987a *J. Phys. C: Solid State Phys.* **20** 879
—— 1987b *Z. Phys.* B **65** 415
—— 1988 *J. Phys. C: Solid State Phys.* **21** 3407
Hofacker I 1990 *Diplomarbeit* TU München, unpublished
Howell F S, Bose R A, Macedo P B and Moynihan C T 1974 *J. Phys. Chem.* **78** 639
Imanishi Y, Adachi K and Kotaka T 1988 *J. Chem. Phys.* **89** 7585
Ishida Y, Matsuo M and Yamafuji K 1962 *Kolloid-Z.* **180** 108
Johari G P 1986 *Polymer* **27** 867
Jonscher A K 1977 *Nature* **267** 673
Kohlrausch R 1854 *Pogg. Ann. Phys.* **51** 56
Krieger U and Bosse J 1987 *Amorphous and Liquid Materials* ed E Lüscher, G Fritsch and G Jacucci (Dordrecht: Martinus Nijhoff) p 139
Leutheusser E 1984 *Phys. Rev.* A **29** 2765
McCrum N G, Read B E and Williams G 1967 *Anelastic and Dielectric Effects in Polymeric Solids* (London: Wiley)
Mezei F, Knaak W and Farago B 1987 *Physica Scripta T* **19** 363
Ngai K L 1979 *Commun. Solid State Phys.* **9** 127
Palmer R G, Stein D L, Abrahams E and Anderson P W *Phys. Rev. Lett.* **53** 958
Pavlatou E A, Rizos A K, Papatheodoru G N and Fytas G 1991 *J. Chem. Phys.* **94** 224
Petry W, Bartsch E, Fujara F, Kiebel M, Sillescu H and Farago B 1991 *Z. Phys.* B preprint
Piazza R, Bellini T, Degorgio V, Goldstein R E, Leibler S and Lipowsky R 1988 *Phys. Rev.* B **38** 7223
De Raedt H and Götze W 1986 *J. Phys. C: Solid State Phys.* **19** 2607
Richter D, Frick B and Farago B 1988 *Phys. Rev. Lett.* **61** 2465
Rössler E 1990 *Phys. Rev. Lett.* **65** 1595
Roux J N, Barrat J L and Hansen J P 1989 *J. Phys.: Condens. Matter* **1** 7171
von Schweidler E 1907 *Ann. Phys.* **24** 711
Sidorovich Y A, Pavlov G N and Marei A I 1974 *Polymer Sci. USSR* **16** 993
Signorini G F, Barrat J L and Klein M L 1990 *J. Chem. Phys.* **92** 1294
Sjögren L 1986 *Phys. Rev.* A **33** 1254
Sjögren L and Götze W 1989 *Dynamics of Disordered Materials* ed D Richter, A J Dianoux, W Petry and J Teixeira (Berlin: Springer) p 18
Williams G and Hains P J 1972 *Faraday Symp. Chem. Soc.* **6** 4
Williams G and Watts D C 1970 *Trans. Faraday Soc.* **66** 80
Wong J and Angel C A 1976 *Glass: Structure by Spectroscopy* (Basel: Marcel Dekker)